CONTRIBUTIONS TO DEVELOPMENT OF A WIND VULNERABILITY MODEL – Final Report 2009-10

CONTRIBUTIONS TO DEVELOPMENT OF A WIND VULNERABILITY MODEL – Final Report 2009-10

J.D. Holmes

(Report prepared for Geoscience Australia)

June 2010

JDH Consulting
Report JDH 10/2

JDH Consulting
P.O. Box 269
Mentone
Victoria
Australia
3194
Ph. 03-9584-5885
FAX 03-9585-3815
e-mail : ***John.Holmes@jdhconsult.com***

1. INTRODUCTION

This report describes contributions by JDH Consulting (JDH) to a Geoscience Australia (GA) project to develop simulation tools to model the vulnerability of Australian building stock to existing and future wind hazards.

The following summarizes the deliverables from JDH required by GA in 2009-10:

1. Provide suites of boundary-layer gust profiles which capture the variability in gust wind speed with height for cyclone and thunderstorm wind events.

2. Provide recommendations for the expected shielding of individual houses within a suburb, and for the differential shielding between different building envelope surfaces.

3. Provide recommendations for a debris damage model, including necessary parameters for GA to develop computer code.

This is the final report on the JDH contributions for 2009-10, and includes variations and adjustments resulting from consultations and workshops held in December 2009 (Canberra), February 2010 (Townsville) and May 2010 (Townsville).

Section 2 following describes the methodology for producing randomized gust profiles, and the resulting profiles (Deliverable 1). Section 3 discusses the variability of the shielding effects (Deliverable 2). Sections 4 to 6 discuss the elements of a debris damage model (Deliverable 3). The report contains several Appendices associated with Deliverables 1 and 3.

2. RANDOMIZED WIND GUST PROFILES

JDH Consulting was requested to provide information to capture the variability with height of wind gust speeds in strong wind events such as tropical cyclones and severe thunderstorm events. This task constitutes 'Deliverable 1' in a number to be undertaken, and is summarized in the Statement of Work defined by GA as below.

Provide suites of boundary layer profiles which capture the anticipated variability in wind speed with height for cyclone and thunderstorm wind events. Ten profiles for each wind event for each of the terrain categories 2, 2.5, and 3 are to be provided. Each profile shall have an equal probability of occurrence in a wind event and be defined by a minimum of ten points with one point at 10m height and at least three points below 10m height.

The above statement refers to wind *gust* profiles (nominally 2-3 second gusts as used in AS/NZS1170.2 [1]), and not wind speeds averaged some longer time period, such as 1 minute or ten minutes. The above statement could be taken to include

simultaneous gust profiles that can be expected to occur during a given wind event, or alternatively, various *envelopes* of non-simultaneous extreme gusts that might occur during any of a set of similar events. The former may be more useful for determining the response of a structure that extends over a significant height range such as a tower. The latter is more appropriate for a variety of low-rise buildings of various height exposed to a given extreme wind event, for which it is assumed that the wind forces and resulting damage are directly related to the peak gust at average roof height (as assumed in the Wind Actions Standard AS/NZS1170.2 [1]). Both types of profiles are addressed in this report and the simultaneous profiles were themselves used to develop envelope profiles.

The ten heights at which wind gust speeds were simulated are as follows:

3, 5, 7, 10, 12, 15, 17, 20, 25, 30 metres above ground level

2.1 Simultaneous gust profiles

The simultaneous gust profiles are based on 'expected' gust profiles based on the following equation:

$$V(z)_{z1\,max} = \bar{V}(z) + g\,\rho_{z,\,z1}\,\sigma_V \qquad (1)$$

where z is the height of the wind gust

z_1 is the 'pivot' height at which the wind gust is stipulated to reach a maximum for a given profile

g is a peak factor taken, for these simulations, as a constant value of 3.7

$\rho_{z,\,z1}$ is the correlation coefficient between wind velocity fluctuations at the two heights z and z_1

Equation (1) is a variation of the well-known LRC formula which is more commonly used to determine effective distributions of wind *pressure* for the response of large structures such as towers and stadium roofs [2]. It gives the expected wind gust speed at height z, when the gust speed is at its maximum at height z_1.

The correlation between velocity fluctuations is assumed to be represented by Equation (2), in which L_{uz} is the vertical integral length scale of the wind speed fluctuations. The latter was assumed to be one half of the longitudinal length scale – i.e. 85/2 = 42.5 m at a height of 10 metres [1].

$$\rho_{z,\,z1} = \exp\left(-|z - z_1|/L_{uz}\right) \qquad (2)$$

Applying Equation (1) ten times with the height, z_1, varying over the height range of 3 to 30 metres, gave ten 'expected' instantaneous profiles each corresponding to a maximum gust at a different height, i.e. the pivot height z_1. These profiles were further 'randomized' by varying the standard deviation by small amounts around its

nominal value. For tropical cyclones, the turbulence intensities given in Table 6.1 in AS/NZS1170.2:2002 [1] were used. The percentage 'randomness' in the standard deviation was arbitrarily chosen as 5% for Terrain Category 2, 7.5% for Terrain Category 2½, and 10% for Terrain Category 3. The variation was assumed to have a Gaussian probability distribution, for which random numbers were generated using the Box-Muller technique. The mean wind speed $\overline{V}(z)$ was obtained using mean terrain-height multipliers from Table 4.2.5.2 in AS1170.2-1989 [3].

Ten simultaneous profiles for tropical cyclones, simulated in this way, are shown in Figures 1 to 3 and tabulated in Appendix A. The nominal maximum gust at 10 metres height in Terrain Category 2 for all these profiles is 70 m/s. It is noted that the turbulence intensities are the same for Terrain Categories 2, 2½ and 3, in both AS/NZS1170.2:2002 [1] and AS1170.2-1989 [3].

Figure 4 shows simultaneous gust profiles for a thunderstorm downdraft simulated in a similar way to that described above. In this case, a uniform 1-minute mean wind speed was assumed above 10 metres with a reduction below 10 metres following that in synoptic winds in Terrain Category 2 according to AS1170.2-1989 (Table 4.2.5.1). A turbulence intensity of 0.10 (10%) was assumed for all heights. The peak factor, g, was taken to be 3.0 – appropriate to the reduced averaging time of 1 minute. The nominal 10 metre maximum gust for this event was taken as 45 m/s. The general characteristics of the downdraft profiles are based on that measured in the rear-flank downdraft in Texas in 2002 [4].

The ten profiles given in Figure 4 are tabulated in Appendix B. The same profiles can be assumed for all terrain categories in this case.

The ten profiles in each of Figures 1 to 4 can be thought of as instantaneous gust profiles at different times in the same event corresponding to each Figure. They are selected random gust profiles associated with the maximum gust in the event occurring at one of the ten heights.

2.2 Randomized gust envelopes

The maximum gust at a height of 10 metres will not, in general, occur at the same time in the same event as that at 20 metres, for example. This can be seen from Figures 1 to 4.

The series of terrain-height multipliers in AS/NZS1170.2:2002 is not a simultaneous gust profile at a point in time, but represents the average *envelope* of maximum gusts at different times in the same severe wind event.

The method used to simulate a series of gust envelope 'profiles' was to generate ten groups of ten profiles such as those shown in Figures 1 to 4. Then the envelope profile (i.e. the largest gust wind speed at each height) from each group of ten formed a single random envelope profile.

Figures 5 to 7 show gust envelope profiles generated as described above for tropical cyclone winds. The values have been normalized by dividing by the value at 10 metres height in each case. Thus the profiles shown are essentially plots of $M_{z,\,cat}$ /$M_{10,cat}$. The values are tabulated in Appendix C. It can be seen that the profiles are steeper and have more variability as the terrain roughness increases – i.e. as the Terrain Category changes from TC 2 to TC2½ to TC3.

Figure 8 shows the normalized envelope profile for thunderstorm downdrafts – assumed to be terrain-independent - derived in the same way. The tabulated values are in Appendix D. These profiles are flat above 10 metres height and have relatively low variability compared to the tropical cyclone winds, due to the effective lower turbulence intensity in thunderstorm events.

2.3 Summary – randomized gust profiles

'Random' gust profiles have been generated for tropical-cyclonic winds for three terrain categories. Ten simultaneous gust profiles have been simulated for each case. Ten gust envelope profiles, which are equivalent to those given in AS/NZS1170.2:2002 [1], have also been simulated using one hundred simultaneous profiles. The gust envelope profiles were normalized to the value at 10 metres height. These profiles are more appropriate for simulations of damage to low-rise buildings, in which the wind pressures and forces can be assumed to be related to the maximum wind gust speed at average roof height.

A similar set of profiles has been generated for downdraft winds. These can be assumed to be terrain independent, as they develop over very short fetch distances; however the characteristics are based on full-scale measurements in an actual severe downdraft event in Texas in 2002.

3. VARIABILITY OF SHIELDING EFFECTS

JDH Consulting was requested to model the variability of shielding multipliers within a suburban area, and also separate the differential shielding for different building surfaces. These tasks constitute 'Deliverable 2', and are summarized below:

2a) Provide recommendations for variation of shielding for individual houses within a level suburb ignoring slope and proximity of suburb edges. i.e. what is the likelihood of an individual structure within a suburb having full, partial or nil shielding.

2b) Provide recommendations for differential shielding between different building envelope surfaces where an individual structure is shielded. i.e. what are the incremental adjustments to be applied to envelope surface pressures to account for different degrees of shielding between envelope surfaces on a single shielded structure.

For the purpose of this study the shielding will be taken to be represented by the 'shielding multiplier', M_S, as defined in the Australian Standard for Wind Actions, AS/NZS1170.2:2002 [1]. This multiplier represents the reduction in peak 3-second gust velocity at a given height and terrain, caused by the presence of buildings and other obstructions upwind of the site of interest. It is a good single indicator of the shielding effect.

3.1 Variation of shielding multipliers – BRE studies

The best source of data available to JDH to directly compute the variability of shielding multipliers in urban areas was the full-scale study carried out by the Building Research Establishment (BRE) in the U.K. in the 1970s ([5], [6], [7]). In particular Reference [6], which contains the raw data obtained by BRE between 1972 and 1974 was used for the present work.

In this study, portable anemometers were located in many urban locations in Hertfordshire, north of London. Examples of some of these are shown in Figure 9. Measurements of wind speeds at three different heights were compared with simultaneous values obtained at 10-metres height in an upwind rural location. Averaging of wind speeds over periods varying from 10-seconds to 10-minutes was carried out.

The velocity ratios obtained in the BRE study were defined as follows:

$$VR = \frac{windspeed\ \ with\ a\ \ t-\text{sec}ond\ \ averaging\ \ time\ at\ \ a\ \ given\ \ height\ and\ \ location}{windspeed\ \ with\ a\ \ t-\text{sec}ond\ \ averaging\ \ time\ at\ \ 10m\ \ height\ in\ \ rural\ \ terrain}$$

Figure 10 shows some histograms of the velocity ratios defined as above. The considerable variability in the values can be noted. It will also be seen that, even at a height of 5m, the ratio occasionally exceeded 1.0 – this implies that a gust or mean wind speed in the urban location was occasionally larger than the equivalent value at 10 m height in open country. However, the average values are comparable to the nominal values ($M_{z,cat}$. M_s) obtained from a standard such as AS/NZS1170.2 [1].

In the absence of equivalent measurements in Australia, the values measured at BRE can be usefully used as an indication of the variability in the shielding obtained in urban areas.

3.2 Mean and standard deviation of shielding multipliers

The shortest averaging time used in the BRE study [6] was 10 seconds. An extrapolation was used to determine the appropriate values of the mean and standard

deviation of the 3-second values required for this study. The following procedure was adopted:

- Mean values of the above ratio (VR) for 5-m height in urban terrain and various values of the averaging time, t, were plotted against $\log_{10} t$ (see Figure 11).
- A line of best-fit was used to extrapolate the mean ratio to a value of t = 3seconds.
- The coefficient of variation of VR was found to be insensitive to the value of t, and an average value – i.e. averaged over all values of t – was obtained.

This procedure resulted in the following mean and coefficient of variation for the 3-second velocity ratio in the U.K. urban situation (5 metres height):

U.K.: Mean value = 0.625
Coefficient of variation = 0.315

The mean 'shielding multiplier' can be obtained by dividing the mean value of the velocity ratio by $M_{5m,Cat3}$ obtained from AS/NZS1170.2 [1] – i.e. a value of 0.83. This gives a mean value of M_s for the U.K. urban situation of 0.75.

In the above procedure, the variability obtained was the combined variability of the product $M_{z,cat}$. M_s, and hence would over-estimate the variability in M_s alone. In order to separate the variability of M_s, it can be assumed that BRE measurements at 10 metres height in urban areas do not include significant shielding effects, and represent the variability only in the gust velocity profile alone – i.e. in $M_{z,cat}$. The BRE values at 10m height for 10-second peaks gave a coefficient of variation of 0.215. Subtracting the square of this value from the square of the combined value of 0.315, and taking the square root gives an estimate of the variability of the shielding multiplier alone:

$$\text{COV } M_s \cong \sqrt{(0.315^2 - 0.215^2)} = 0.23$$

The UK urban situation consisted primarily of 2-storey continuous terraces or duplex buildings. In Australia houses are more likely to be single storey, and are generally more widely spaced than in urban areas in south-east England. Hence, shielding multipliers are likely to be lower on average in Australia compared to the U.K.

Hence the following values of mean and coefficient of variation are recommended as appropriate ones for shielding multipliers in 'typical' Australian conditions (i.e. outer suburbs and country towns):

Australia: Mean value of M_s = 0.85
Coefficient of variation of M_s = 0.23

3.3 Probability distributions and shielding categories

The shielding multipliers can be assumed to have either a normal or a lognormal probability distribution. The normal distribution is symmetrical about the mean value, but has a disadvantage that it can take negative values; the lognormal distribution cannot take negative values, but is skewed and has a longer 'tail'.

AS4055 ('Wind loads for housing') [8] defines the shielding multiplier for 'full', 'partial' and 'no' shielding as 0.85, 0.95 and 1.0 respectively. These are nominal values used for code purposes. For the present purposes the shielding multiplier is assumed to fall within the following ranges:

'Full shielding' : $M_s \leq 0.9$
'Partial shielding' : $0.9 < M_s < 1.00$
'No shielding' : $M_s \geq 1.00$

Assuming a mean value of 0.85 and coefficient of variation of 0.23 and either a normal or lognormal distribution, the fraction of occurrences within the ranges above have been calculated and are tabulated in Table I.

Table I.

Type	Range	Fraction (lognormal)	Fraction (normal)
Full shielding	$M_s \leq 0.9$	0.652	0.611
Partial shielding	$0.9 < M_s < 1.00$	0.139	0.160
No shielding	$M_s \geq 1.00$	0.210	0.229

It can be seen from Table I, that the assumption made for the probability distribution only changes slightly the distribution of occurrences between 'full' and 'partial' shielding, and has little effect on the fraction judged to have 'no' shielding.

Based on the above studies of urban wind gust velocities, the following percentages are recommended for the shielding of houses well inside Australian urban areas:

Full shielding: 63%

Partial shielding: 15%

No shielding: 22%

3.4 Differential shielding effects

A comprehensive study of wind pressures on grouped houses at James Cook University in the late 1970s [9] provides a useful source to determine the differential shielding effects on various building surfaces. This work consisted of point pressure

measurements on models of low-set and high-set houses, surrounded by rows of similar buildings, in a boundary-layer wind tunnel (Figure 12). A large number of combinations of upwind and downwind rows and building spacings were studied. The study found different reductions in mean and peak pressures, due to shielding, for surfaces such as windward walls, upwind roof and downwind roof.

An analysis of the reduction in local peak pressures is given in Tables II and III following, for building spacing of 40 metres and 20 metres respectively. The former spacing is typical of outer suburban areas and smaller country towns, and the latter of inner suburban areas of larger cities. The Tables give average ratios of peak pressures (maximum pressure for the windward wall, and minimum pressures for all other surfaces) for cases in which there was at least one row of shielding, to the peak pressures on buildings for which there was no shielding row present. In the case of the high-set buildings, shielding was provided by other high-set houses of equal height. For the low-set (single-storey) buildings shielding was provided either by rows of other low-set buildings of equal height, or by high-set houses of greater height.

Table II – Average peak pressure reduction due to shielding – 40 m building spacing

Surface	High-set buildings	Low-set buildings
windward wall	0.98	1.04
side walls	1.04	0.91
leeward wall	1.05	0.90
upwind roof – l.e.	0.67	0.87
upwind roof – centre	0.81	1.04
upwind roof – ridge	0.82	1.01
downwind roof – ridge	0.96	1.03
downwind roof – remainder	0.93	0.99

Table III – Average peak pressure reduction due to shielding – 20 m building spacing

Surface	High-set buildings	Low-set buildings
windward wall	0.94	0.83
side walls	0.85	0.61
leeward wall	0.70	0.86
upwind roof – l.e.	0.47	0.48
upwind roof – centre	0.57	0.60
upwind roof – ridge	0.72	0.75
downwind roof – ridge	0.90	0.87
downwind roof – remainder	0.77	0.83

Table II shows that the only significant reduction in peak pressures with shielding buildings at 40 metre spacing, occurs on the upwind roof, with virtually no shielding effects on the other surfaces, and in some cases slight increases in peak pressures.

However when the building spacing is reduced to 20 metres (Table III) the reductions are significant on all surfaces, with peak pressures being more than halved for the leading edge strip along the upwind roof.

The differing values for different building surfaces in Tables II and III are in contrast to the prediction of AS/NZS1170.2 [1] which give a single shielding multiplier, M_s, and implies a uniform pressure ratio of M_s^2 for all surfaces on a given building.

Based on the values in Tables II and III, the following recommendations for differential shielding for buildings deemed to be subject to 'full shielding' are made:

For outer suburban situations and country towns:
Neglect shielding effects – except for the leading edges of upwind roofs. For the latter an implied pressure ratio of M_s^2 (equal to 0.85^2 for the full shielding cases, and 0.95^2 for partial shielding cases) can be adopted.

For inner suburban buildings with 'full shielding':
Reduce the shielding multiplier to 0.7 for upwind roof areas, except adjacent to the ridge (implying a pressure reduction factor of 0.49).
Retain a nominal value of M_s of 0.85 for all other surfaces.

For inner suburban buildings deemed to have 'partial shielding':
Reduce the shielding multiplier to 0.8 for upwind roof areas, except adjacent to the ridge (implying a pressure reduction factor of 0.64).
Retain a nominal value of M_s of 0.95 for all other surfaces

4. DEBRIS DAMAGE MODEL

A report for GA [10] reviewed previous work on windborne debris and discussed the basic components of a windborne debris model, as applied to tropical housing in Australia.

Probabilistic, engineering debris damage models have been described previously by Twisdale *et al*. [11] and Lin and Vanmarcke [12]. Ideas and methods from these references have been incorporated into the following model proposals where appropriate.

The main elements of a debris damage model can be summarized as follows:

- ***A debris generation module***
- ***A debris trajectory module***
- ***A debris impact module***

These three components will be analyzed in more detail and flow charts and appropriate probability distributions outlined, for implementation by GA, as part of the overall wind damage modeling.

4.1 Debris generation module

Within the debris generation stage, the following steps should be implemented.

- *Define a debris generation region for a building*.

This can be taken as 20 times the target building height upwind, and within a 45 degree angular sector (as used in AS/NZS1170.2 [1] for shielding). It is considered unlikely that debris from the roof of a low-rise building, even in a tropical cyclone, will travel more than about 100 metres horizontally, without hitting either the ground or another building. That distance is 20 times the average roof height of a two-storey building.

- *Number of debris items generated*

Windborne debris from a roof will be generated when the local wind speed is sufficiently high a) to produce a structural failure of a cladding element or its fastening, and b) to generate aerodynamic forces exceeding those of gravity and thus initiate flight. It can probably be assumed that if the wind speed is high enough for (a) to occur, then (b) will also occur. Thus the generation of debris may be associated with the failure of roof elements and hence related directly to a wind load/pressure vulnerability model. However a simplified version can be implemented for roof elements only based on the simple heuristic vulnerability curves already developed by GA.

For the number of debris items, a factor f will be required. This is a constant of proportionality relating the average number of debris items associated with a damage increment on the vulnerability curve.

$$\text{i.e.} \quad \Delta \nu_V = f.\Delta D \tag{3}$$

where $\Delta \nu_V$ is the incremental number of debris items generated in a single wind velocity increment – i.e. between two discrete wind velocities. Similarly, ΔD is the increment in wind damage produced by the same increment in wind speed.

.

If structural and cladding damage is produced whenever the wind load acting on it exceeds its resistance, and time history (i.e. fatigue) effects are ignored, then windborne debris items will be generated whenever a local peak gust attains a threshold value. In this scenario, there will be no time dependency on the number of debris items generated. Thus a thunderstorm, lasting a few minutes, might be assumed to generate a similar amount of debris as a weak tropical cyclone lasting

several hours with the same maximum wind gust. However, this may not be a good assumption if fatigue failures are significant (as occurred with steel roofing in Cyclone 'Tracy').

With the time-independent assumption the parameter f in Equation (3) will not be time dependent. It is the estimated total number of debris items generated from each source building when its damage index reaches unity. It will thus be a large number – probably of the order of 100 to 200.

Another way of expressing Equation (3) is as follows.

$$\frac{d\nu}{dV} = f.\frac{dD}{dV} \tag{4}$$

Equation (4) postulates that the rate of generation of debris with respect to the wind speed is proportional to the slope, or derivative, of the vulnerability curve of the source building. For a typical 'S-shaped' vulnerability curve, the derivative will have a maximum at some wind speed. Physically, this implies that the debris generation reaches a maximum at some wind gust speed associated with the highest rate of increase of building damage. As the wind speed increases above this value, the rate of debris generation falls, as the amount of roofing material on the source building available to form debris becomes depleted.

The number of debris items generated by potential source buildings upstream at each wind speed increment should be treated as a random variable with a Poisson Distribution [12]. The mean value of the number of debris items generated at each wind speed increment is $\Delta\nu_V$, which can be determined as described above.

- *Define debris types*.

It should be assumed that damaging windborne debris will be generated from the roof of low- to medium-height buildings. It is recommended that for ease in calculating lift-off and trajectories, that debris be chosen as one of the three generic types proposed by Wills *et al.* [13]: i.e. 'compact' type, 'plate' or 'sheet' type and 'rod' type. The fractional contributions of each type should be varied depending on the urban environment generating the debris. Table E1 in Appendix E gives suggested fractions within the generic classifications for various Australian situations.

- *Define debris mass and frontal area.*

The debris mass and frontal area will define the flight characteristics at a given wind speed (through the Tachikawa Number [14]). These parameters should be treated as random variables – it is recommended that lognormal probability distributions be used for both these parameters. Suggested values of mean and coefficient of variation are given in Appendix E.

A flow chart for a debris generation module is given in Appendix F.

4.2 Debris trajectory module

Detailed studies of debris trajectories have indicated that the ratio of horizontal velocity of the windborne debris object to the wind gust velocity can be directly related to the horizontal distance travelled, x, by the following ([10], [15]):

$$\frac{u_m}{V_s} \cong 1 - \exp\left[-b\sqrt{x}\right] \tag{5}$$

where u_m is the horizontal velocity of the debris object
V_s is the local (gust) wind speed
x is the horizontal distance travelled
b is a dimensional parameter depending on the shape of the object and its drag coefficient, and its mass:

$$b = \sqrt{\frac{\rho_a C_{D,av} A}{m}} \tag{6}$$

where ρ_a is the air density
$C_{D,av}$ is an average drag coefficient (averaged over all rotations during flight)
A is the frontal area
m is the mass of the object

Eq. (5) is an empirical expression and both experimental data (small scale in wind-tunnel studies) and numerical simulations indicate variability around a mean value. The latter, however, can be represented well by Eq (5).

The following values of $C_{D,av}$ in Eq. (6) are suggested for various generic debris types:

Compact: ***0.65***
(this is an average value based on measured values for spheres and cubes [15])

Sheet/plate type: ***0.90***
(based on measurements described by Lin *et al.* [16])

Rod type: ***0.80***
(based on measurements and numerical simulations described in [15])

Lin and Vanmarcke [17] have suggested that the ratio of missile speed to wind gust speed be modeled as a random variable with a Beta distribution, which can only take values between 0 and 1. The mean value is assumed to be given by Eq. (5).

Equation (7) gives the equation for the p.d.f. for this distribution which involves the Gamma function Γ( ), and two parameters denoted by a and b.

$$f_Y(y) = \frac{y^{a-1}.(1-y)^{b-1}}{B(a,b)} \qquad (7)$$

where the Beta Function, B(a,b) = Γ(a).Γ(b) / Γ(a+b)

This distribution is shown plotted in Figure 13 for three different pairs of values for the parameters a and b. When a and b are equal, the distribution is symmetrical about the variate, x, equal to 0.5.

The mean value of (u_m / V_s) be taken as the right hand side of Eq. (5). The mean value of the distribution is also given by a/(a+b). A dispersion parameter η equal to (a+b) is then chosen to be the larger of 1/m and 1/(1-m) plus a constant, which was taken as 3. These relationships allow the parameters a and b to be determined for a particular debris item.

A flow chart for debris trajectories is given in Appendix G.

4.3. Debris impact and damage module

The probabilistic debris impact/damage model used in HAZUS-MH [18] was previously described in Ref. [11]. This was a simplified approach for the 'fast-running' software that made use of multiple generic simulations. A slightly different approach based on that given by Lin and Vanmarcke [12] is now suggested here.

The proportion of missiles of a given type that impact on a downwind building needs to be determined. The following approach is suggested for this project.

Following Reference [12], the probability distribution of the point of landing of the debris in a horizontal plane can be described by a bivariate Gaussian Distribution :

$$f_{x,y}(x,y) = \frac{1}{2\pi\sigma_x\sigma_y}\exp\ -\left[\frac{(x-d)^2}{2\sigma_x^{\ 2}} + \frac{(y)^2}{2\sigma_y^{\ 2}}\right] \qquad (8)$$

where x and y are the coordinates of the landing position of the debris assumed as random variables, (x is along the mean wind direction)

d is the mean or expected landing position

σ_x, σ_y are the assumed standard deviations for the coordinates of the landing position.

Information on the parameters for the above distribution is available from wind-tunnel studies and/or numerical simulations. The mean landing position, d, can be related to an assumed time of flight, as used by Lin and Vanmarcke [12].

By sampling from the above distribution, simulations of the landing point of each simulated debris item can be made. If the landing point so sampled falls within the footprint of the target building, then it can be assumed that an impact has occurred, and an increment made to the count of impacts, N_V, for a given gust wind speed.

The final stage is to establish the material damage resulting from impacts of debris objects with known mass, horizontal velocity, momentum and kinetic energy.

Lin and Vanmarcke [12] derived the following equation for the probability of debris damage to a house j amongst a group of houses.

$$P_D = 1 - \exp\left\{-q_j.\alpha(j)\right\} \tag{9}$$

where q_j is the ratio of the vulnerable area (e.g. glazed area) of the building envelope to the total area of the envelope, and $\alpha(j)$ is the mean total number of impacts over the defined damaging threshold produced by debris from other buildings within the group considered. $\alpha(j)$ depends on the number of debris items of various defined types generated by the N houses in the group and on the probability distribution of landing points of debris. As indicated previously, the latter was assumed by Lin and Vanmarcke [12] to be bi-variate Gaussian. These authors assumed a lognormal distribution for the conditional probability distribution of the impact momentum exceeding the failure threshold.

The HAZUS model [18] (also discussed in [11]) uses the following equation for estimating the risk of damage from debris impacts:

$$P_D = 1 - \exp\left\{-N.A.T\left[1 - F_\xi\left(\xi_D\right)\right]\right\} \tag{10}$$

where P_D is the risk of damage due to impacts on a given surface during a time period, T, in a given storm,

N is the average number of impacts per unit time, per unit surface area,
A is the area of the surface,
$F_\xi(\xi)$ is the cumulative distribution of energy or momentum,
ξ_D is the threshold of momentum or energy for damage of the material of that surface.

For a given gust wind speed, N was determined by simulation of generic random debris trajectories. A was taken as equal to the area of glazing on the windward wall(s) of the target building.

Equations (9) and (10) are quite similar and are both based on the Poisson distribution for debris impacts, (Eq.(10) was derived in the previous report [10]).

Combining Equations (9) and (10):

$$P_D = 1 - \exp\left\{- N_V . q . A \left[1 - F_\xi\left(\xi_D\right)\right]\right\} \qquad (11)$$

N_V is the average number of impacts per unit time on the building footprint for wind speed, V
q is the vulnerable fraction of the building envelope
A is the total area of the building envelope
$F_\xi(\xi)$ is the cumulative distribution of impact momentum

It is recommended that Eq. (11) be used to calculate the damage probability. A flow chart for debris impact simulation, and damage estimation is given in Appendix H.

However, an alternative approach would be to count damaging impacts by sampling and simulation.

Although Equation (11) gives the probability of damage it does not *quantify* the damage produced in dollar terms. There is also the consequential damage to consider – i.e. a glass window failure may result in high internal pressures and consequent roof failure.

4.4. Threshold for damage at impact

Information on the threshold of momentum or energy for damage, ξ_D, for various building materials, including glass, was given in an earlier report [10]. The thresholds of momentum for 6mm glass of various types are reproduced in Table IV derived from a paper by Minor [19].

Table IV. Threshold of momentum for failure of 6mm thick glazing [20]

Type of glass	Impact velocity (m/s)	Impact momentum (Kg.-m/s)
annealed	10	0.05
heat strengthened	12	0.06
fully tempered	20	0.10

However the failure momentum should also be treated as a random variable. Lin and Vanmarcke [12] suggested a lognormal distribution with a coefficient of variation of 0.1 (10%) for the impact momentum for failure. Use of a Weibull distribution is another possibility.

4.5. Summary

A skeleton for a windborne debris damage simulation model has been outlined. Methodologies, including flow charts, have been provided for a debris generation module, a debris trajectory module, and a debris impact and damage module. Appropriate probability distributions, mean values and coefficients of variation have been suggested. It has been assumed that Monte Carlo simulation techniques, in which values of each parameter are randomly sampled from the assumed distribution, will be adopted. The final calculation of probability of damage produced may be done by application of Equation (11).

5. CONCLUSIONS

This report has described several tasks carried out by JDH Consulting to assist Geoscience Australia to develop a vulnerability model for wind loads in Australia. These tasks relate to gust profiles in the wind, shielding effects and modelling of the damaging effects of windborne debris in severe windstorms.

The results of all the work described in this report have now been taken up by GA and incorporated into the WindSim damage prediction model.

J.D. Holmes, Ph.D, F.I.E.Aust., C.P.Eng

15 June 2010

REFERENCES

1. Standards Australia. Structural design actions. Part 2: wind actions. Australian/New Zealand Standard, AS/NZS1170.2:2002.

2. Holmes, J.D. and Kasperski, M. (1996). Effective distributions of fluctuating and dynamic wind loads. *Civil Engineering Transactions, Institution of Engineers, Australia,* Vol. CE38, pp83-88.

3. Standards Australia. SAA Loading Code. Part 2: Wind loads. Australian Standard, AS1170.2-1989.

4. Holmes, J.D., Hangan, H., Schroeder, J., Letchford, C.W., and Orwig, K.D. (2008). A forensic study of the Lubbock-Reese downdraft of 2002, *Wind and Structures*, Vol. 11, pp 137-152.

5. Buller, P.S.J. (1974). Wind speeds measured within an urban area – Report Number 1. *Building Research Establishment (U.K.),* Note N26/74, B.R.E. Watford, England, U.K.

6. Buller, P.S.J. (1976). Wind speeds measured within an urban area – Report Number 2. *Building Research Establishment (U.K.),* Note N12/76, B.R.E. Watford, England, U.K.

7. Eaton, K.J. and Buller, P.S.J. (1974). Wind speeds measured in urban areas with anemometers on portable masts, *Building Research Establishment (U.K.),* CP 71/74, B.R.E. Watford, England, U.K.

8. Standards Australia. Wind loads for housing. Australian Standard, AS4055-2006.

9. Holmes, J.D. and Best, R.J. (1979). A wind tunnel study of wind pressures on grouped tropical houses, James Cook University, Wind Engineering Report 5/79, Report for Australian Housing Research Council.

10. J.D. Holmes, Windborne damage debris model for tropical residential construction, JDH Consulting Report JDH 08/2, report prepared for Geoscience Australia, February 2008.

11. L.A. Twisdale, P.J. Vickery and A.C. Steckley, Analysis of hurricane windborne debris impact risk for residential structures, Report prepared for State Farm Mutual. Applied Research Associates, Raleigh, North Carolina, Report 5303. March 1996.

12. N. Lin and E. Vanmarcke, Windborne debris risk assessment, *Probabilistic Engineering Mechanics*, Vol. 23, pp 523-530, 2008.

13. J.A.B. Wills, B.E. Lee, and T.A. Wyatt, A model of windborne debris damage. *Journal of Wind Engineering and Industrial Aerodynamics*, Vol. 90, pp. 555-565, 2002.

14. J.D. Holmes, C.J. Baker and Y. Tamura, The Tachikawa Number – a proposal, *Journal of Wind Engineering and Industrial Aerodynamics*, Vol. 94, pp 41-47, 2006.

15. N. Lin, J.D. Holmes and C.W. Letchford, Trajectories of windborne debris and applications to impact testing. *Journal of Structural Engineering* (ASCE), Vol 133, pp 274-282, 2007.

16. N. Lin, C.W. Letchford and J.D. Holmes, Investigation of plate-type windborne debris. I. Experiments in wind tunnel and full scale, *Journal of Wind Engineering and Industrial Aerodynamics*, Vol. 94, pp 51-76, 2006.

17. N. Lin, E. Vanmarcke, Windborne debris risk analysis – Part 1. Introduction and methodology. *Wind and Structures*, Vol. 13, pp 191-206, 2010.

18. Federal Emergency Management Administration (FEMA), Multi-hazard estimation methodology – Hurricane Model. HAZUS-MH-MR3 Technical Manual. Chapter 5 – Windborne Debris. (available for free download from: www.fema.gov/plan/prevent/hazus/hz_manuals).

19. J.E. Minor, Windborne debris and the building envelope. *Journal of Wind Engineering and Industrial Aerodynamics*, Vol. 53, pp 207-227, 1994.

ACKNOWLEDGEMENTS

The cooperation of Martin Wehner, Mark Edwards and Carl Sandland of Geoscience Australia during the course of this project is gratefully acknowledged.

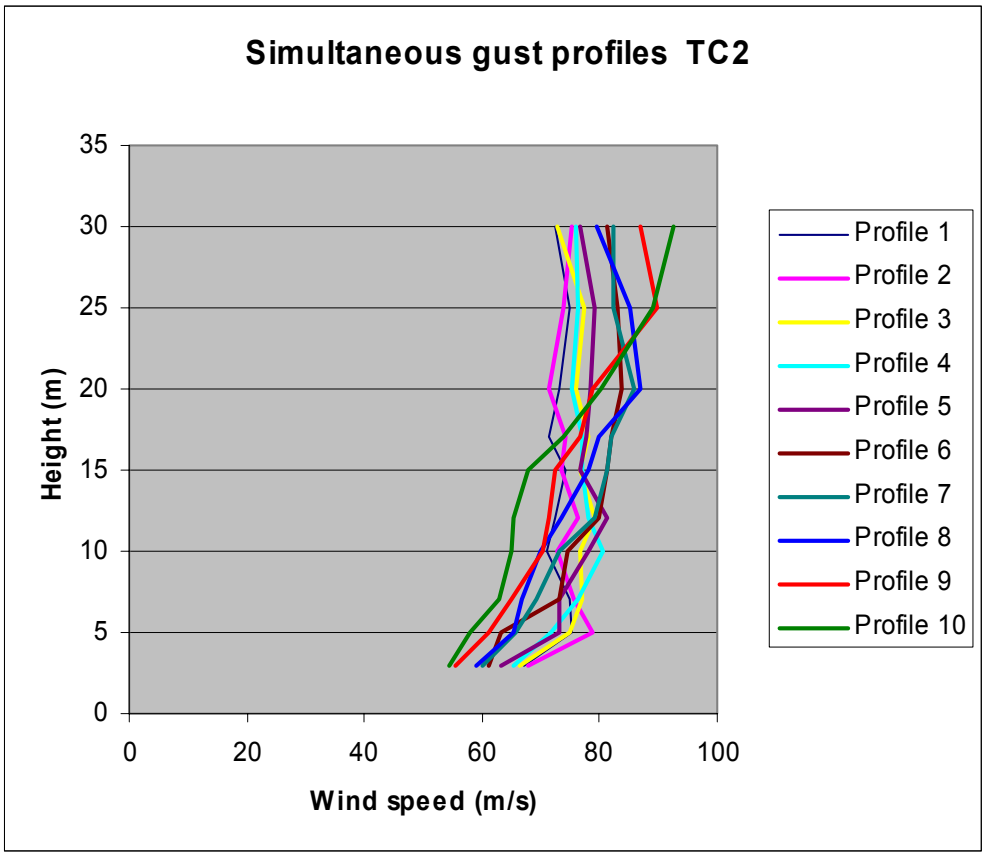

Figure 1. Simultaneous gust profiles in tropical cyclones - Terrain Category 2

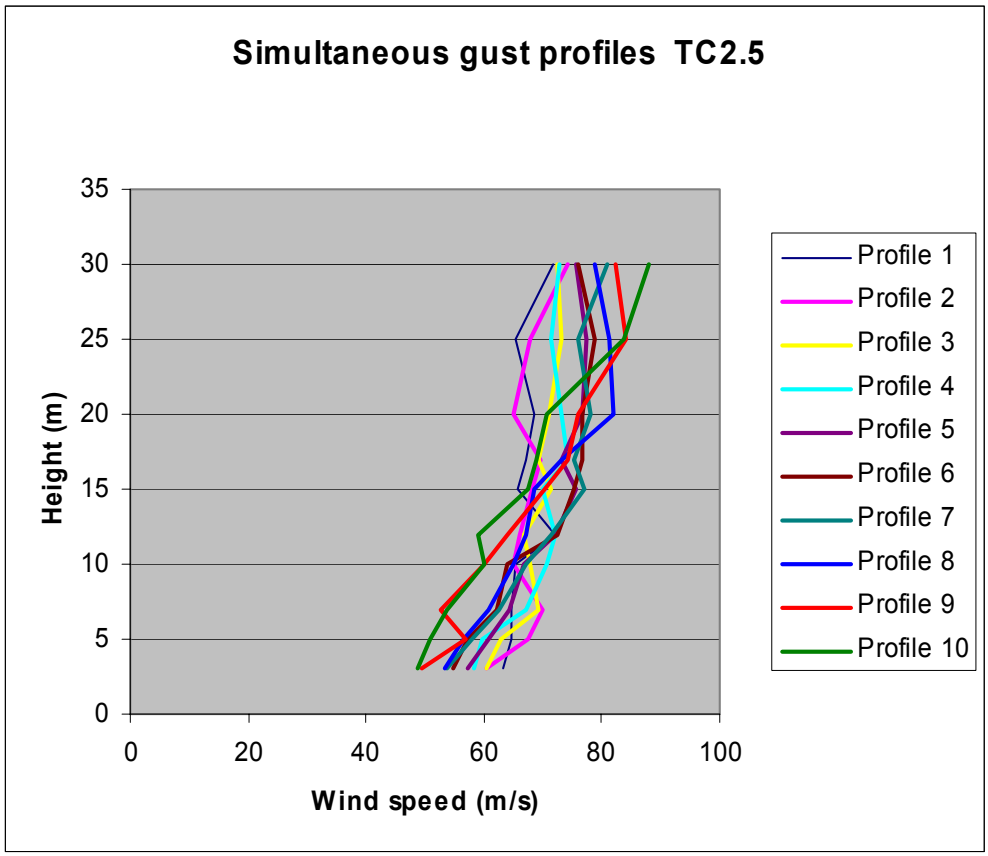

Figure 2. Simultaneous gust profiles in tropical cyclones - Terrain Category 2.5

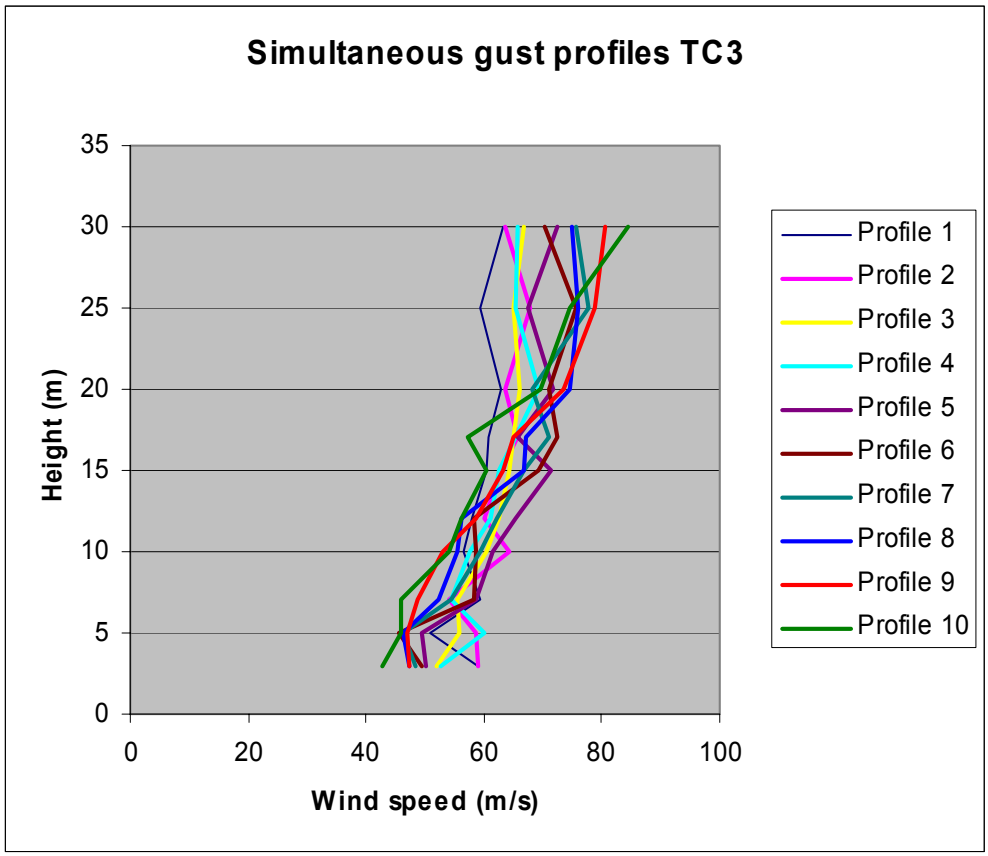

Figure 3. Simultaneous gust profiles in tropical cyclones - Terrain Category 3

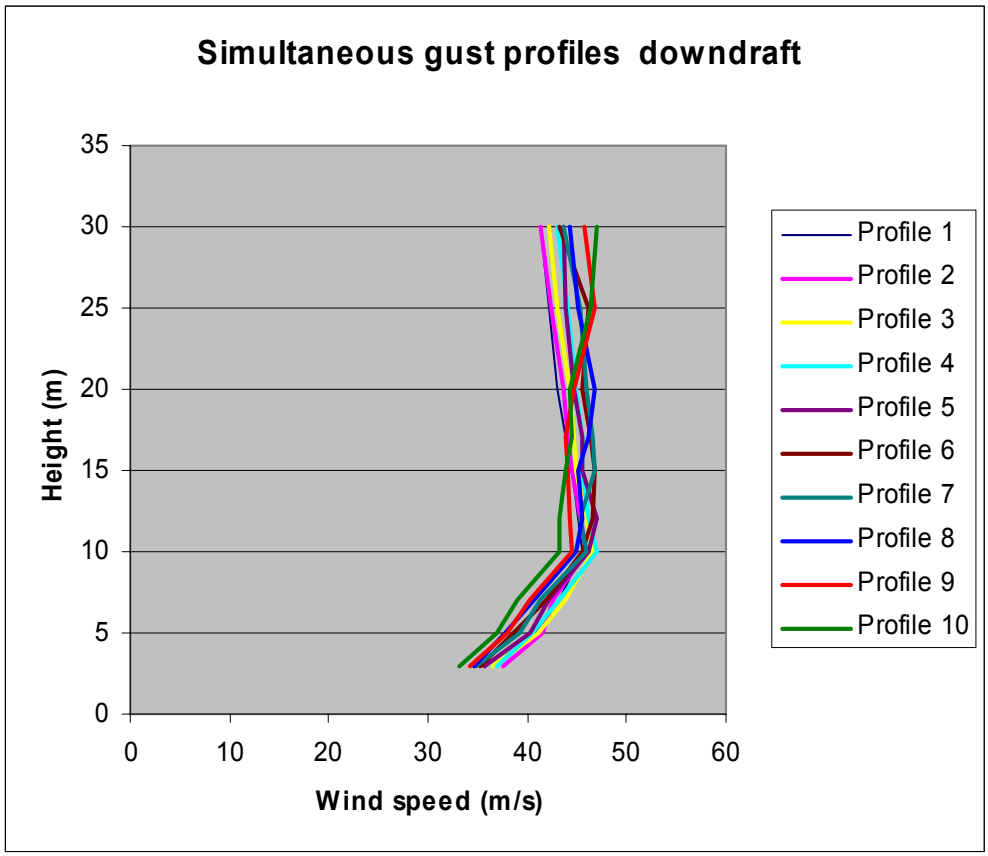

Figure 4. Simultaneous gust profiles in a thunderstorm downdraft outflow (all terrains)

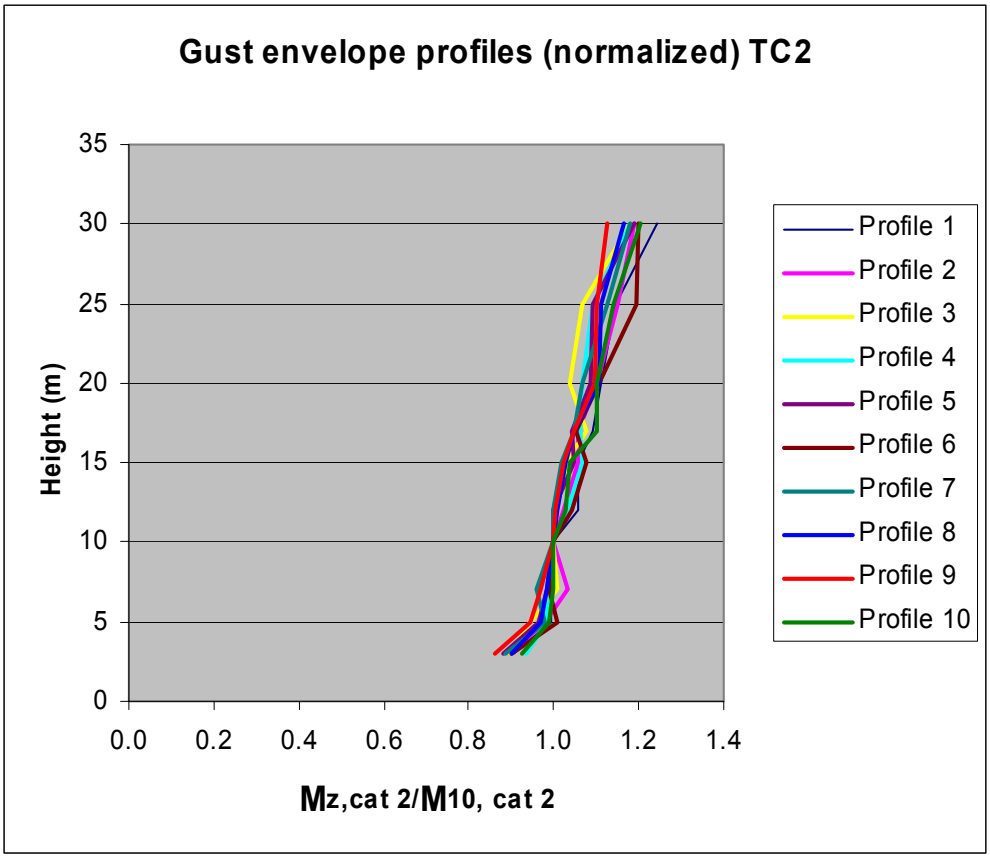

Figure 5. Gust envelope profiles for tropical cyclones - Terrain Category 2

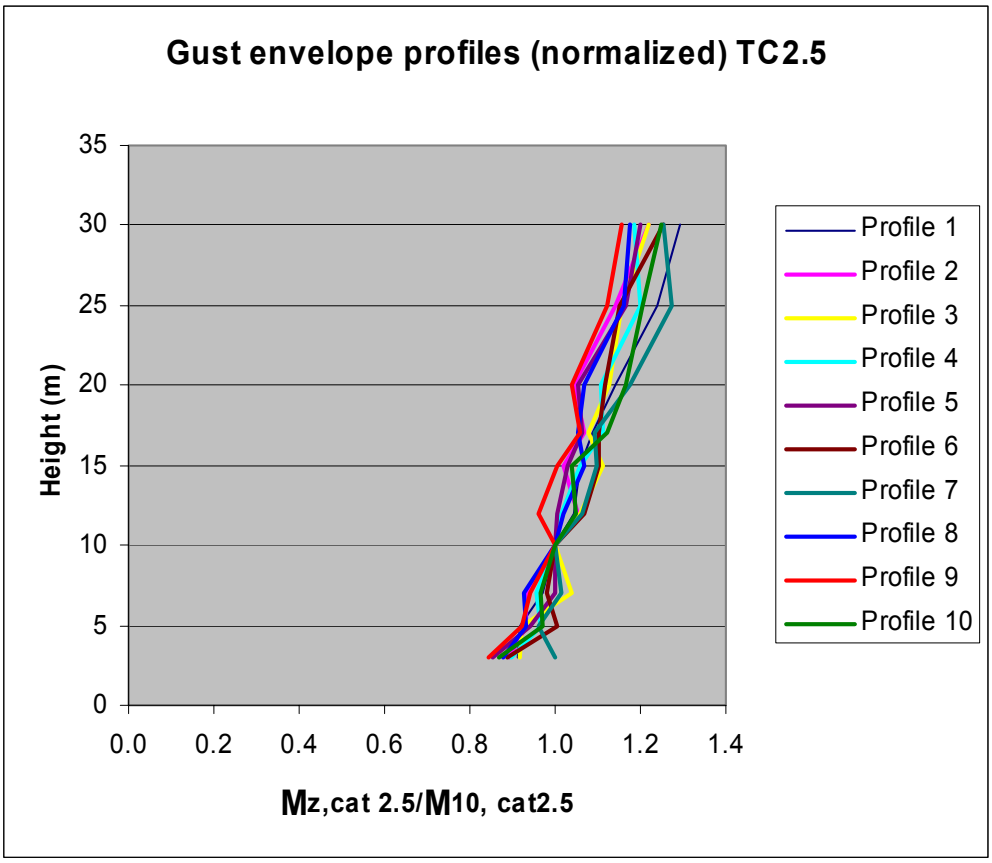

Figure 6. Gust envelope profiles for tropical cyclones - Terrain Category 2½

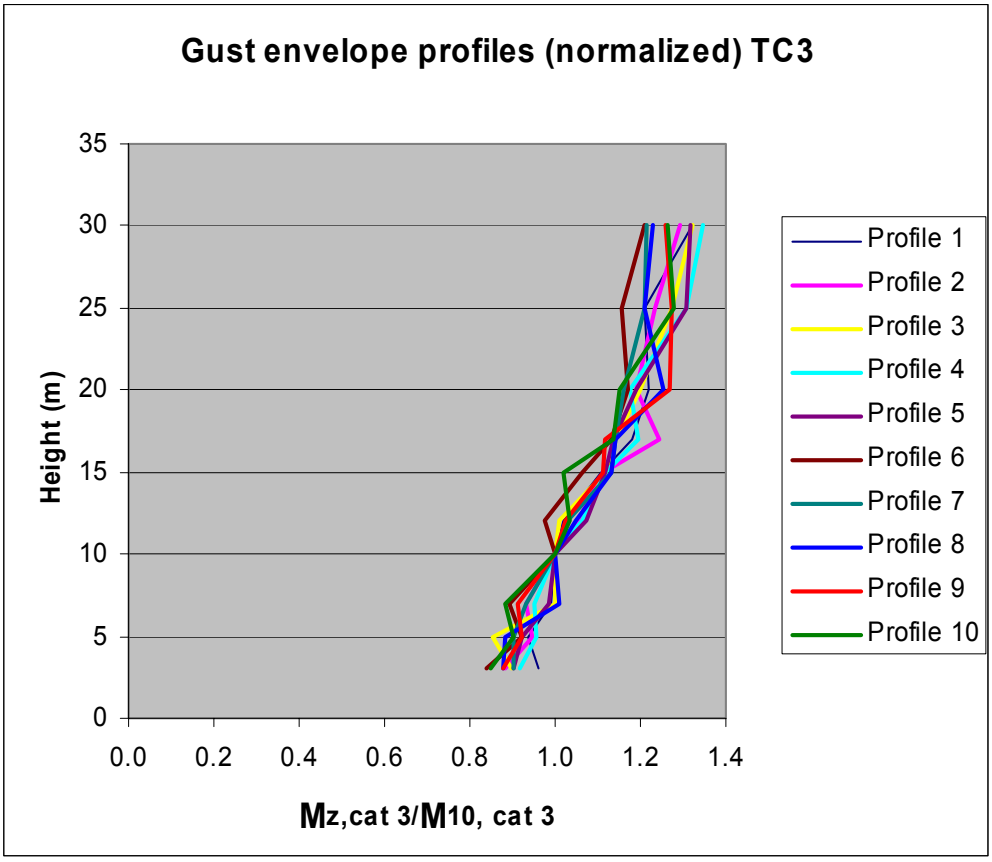

Figure 7. Gust envelope profiles for tropical cyclones - Terrain Category 3

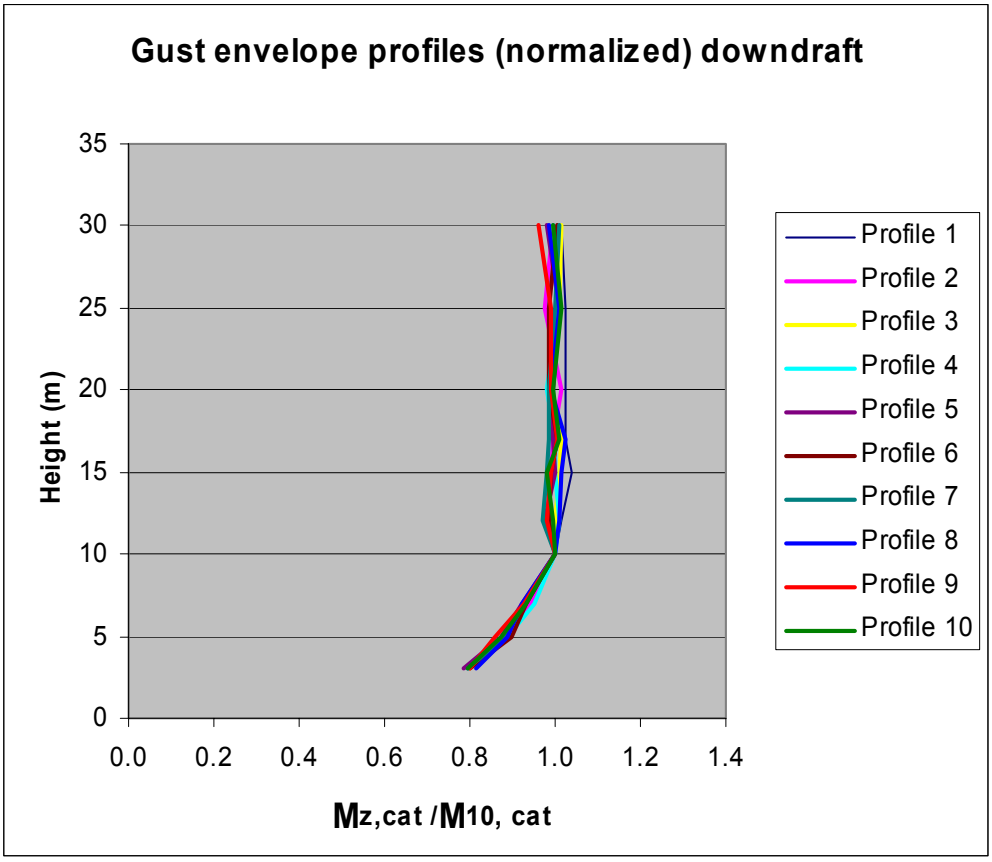

Figure 8. Gust envelope profiles for thunderstorm downdraft outflows – all terrains

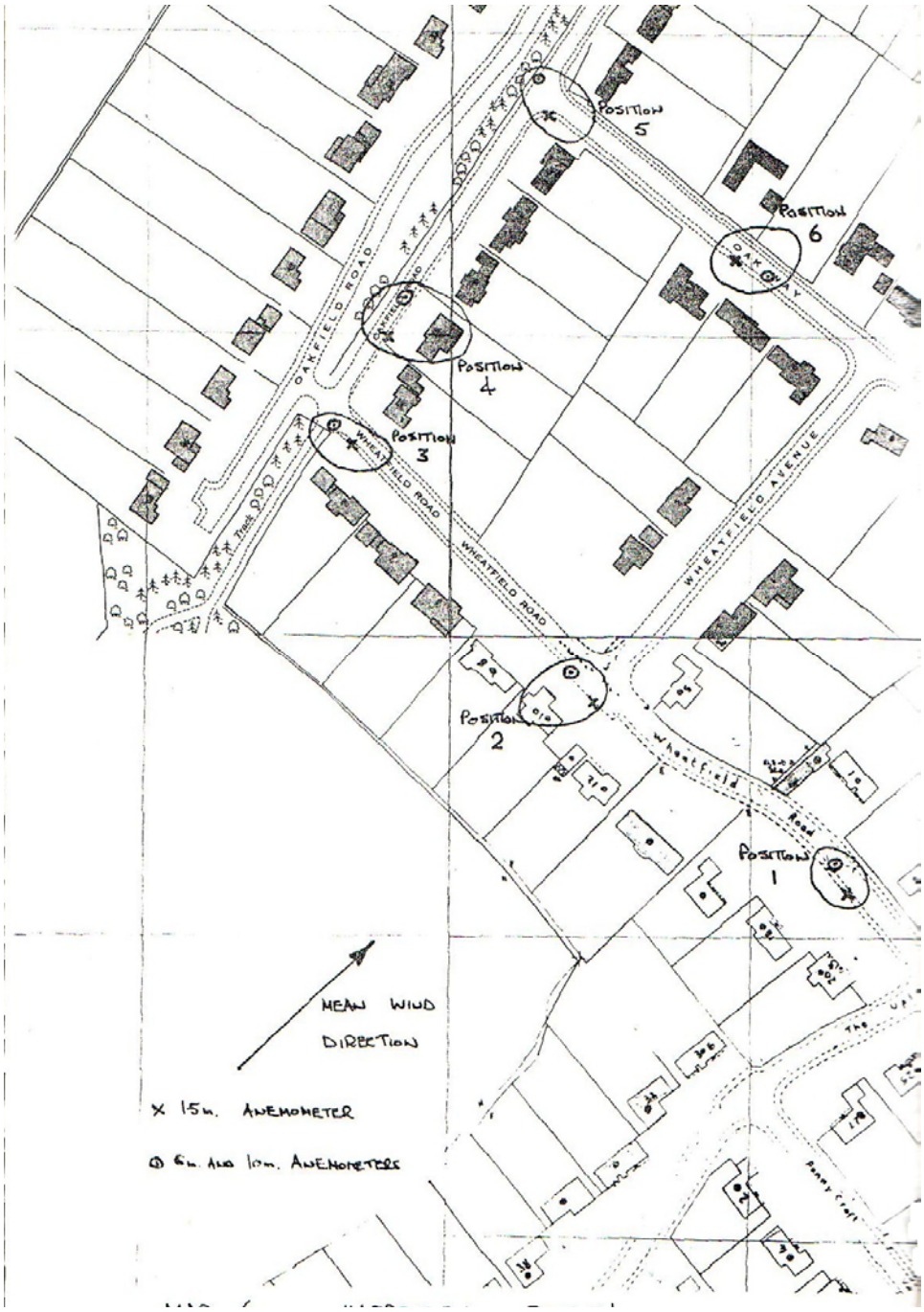

Figure 9. Some anemometer locations for the BRE study 1972-4

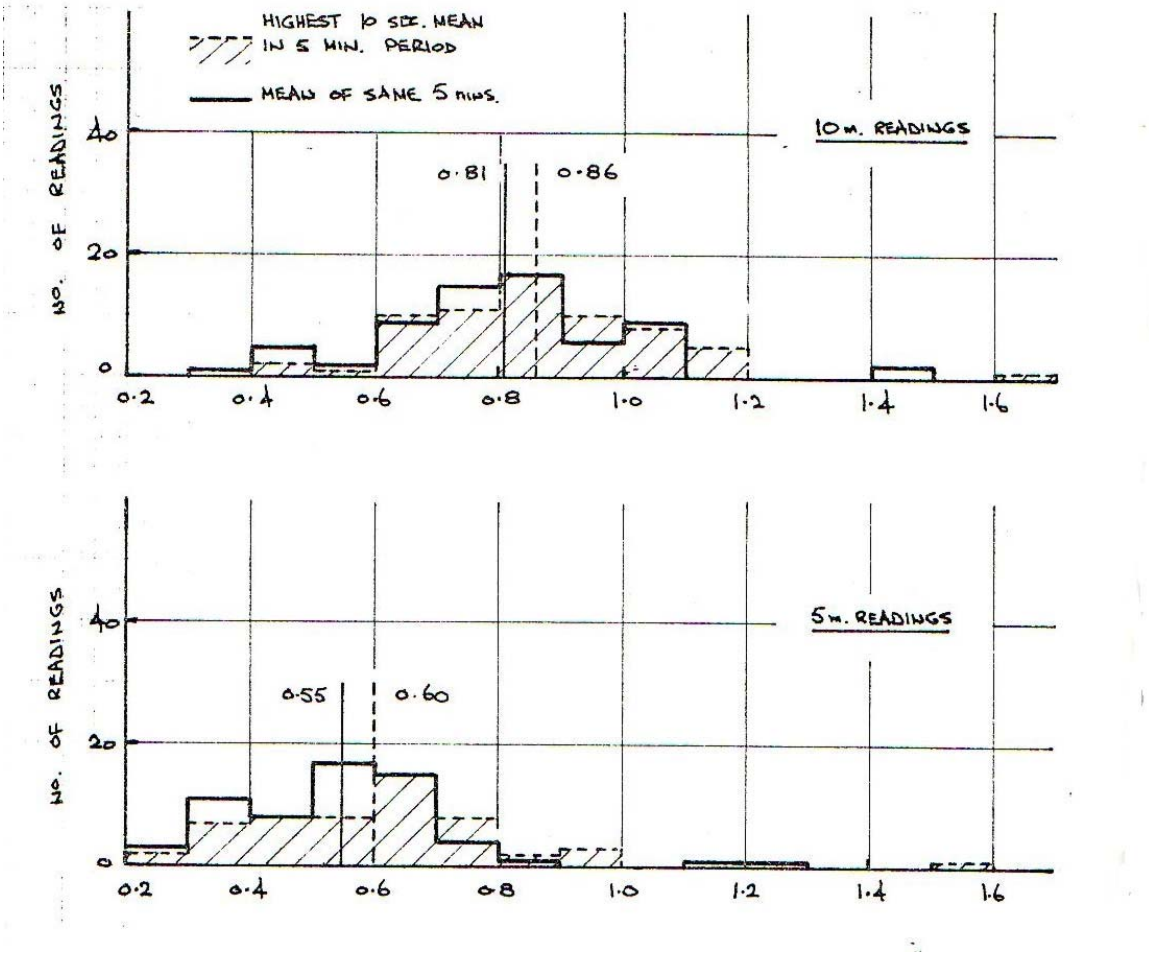

Figure 10. Histograms of velocity ratios in urban locations [6]

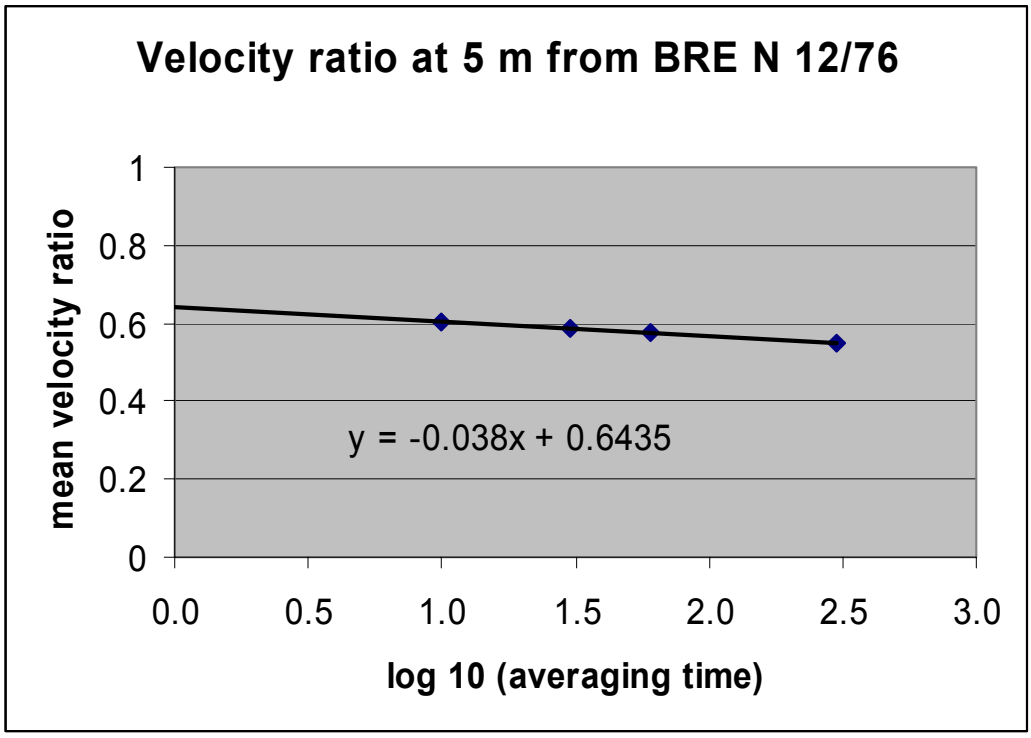

Figure 11. Velocity ratios measured by B.R.E. at 5 m in urban locations

Figure 12. A configuration of grouped houses in the JCU wind tunnel

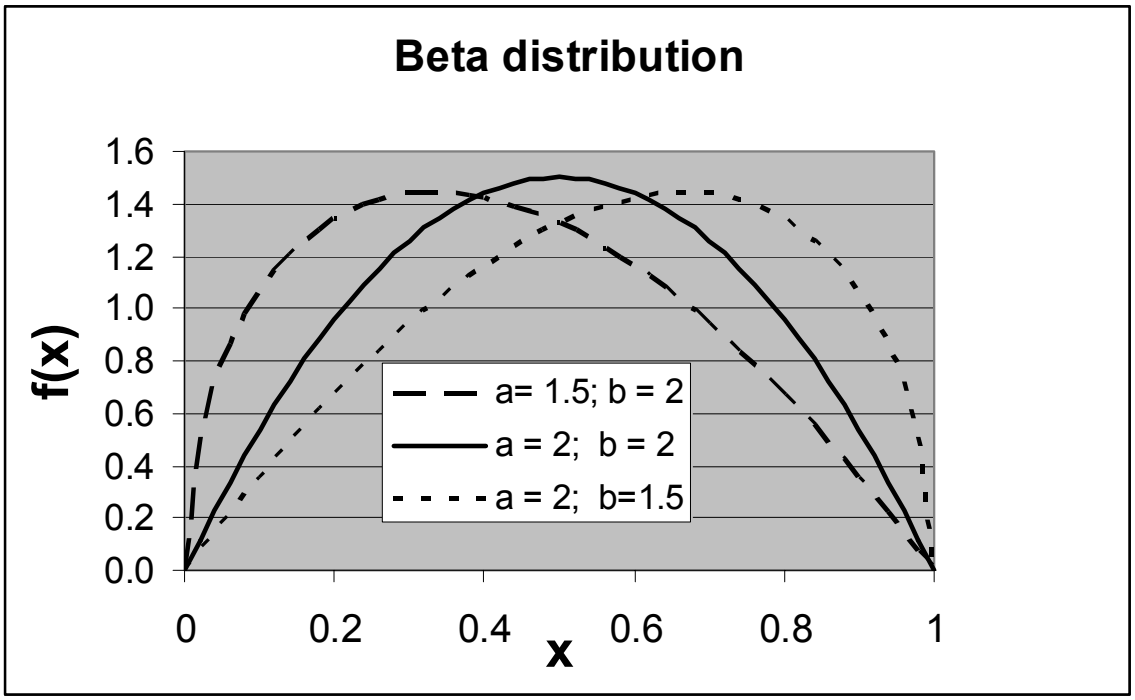

Figure 13. Beta distribution for three different pairs of parameters

APPENDIX A

SIMULTANEOUS GUST PROFILES – TROPICAL CYCLONE

Table A1. Gust profiles - Terrain Category 2

Height m	Profile 1	Profile 2	Profile 3	Profile 4	Profile 5	Profile 6	Profile 7	Profile 8	Profile 9	Profile 10
3	67.19	67.83	66.40	65.35	63.16	61.24	60.09	59.03	55.31	54.56
5	75.12	78.88	74.82	71.80	73.20	63.37	65.76	65.20	61.17	57.79
7	75.04	75.62	77.14	76.16	73.31	73.09	69.42	66.95	65.16	63.05
10	70.88	72.64	76.51	80.60	78.09	74.65	72.98	69.84	70.31	65.08
12	72.28	76.36	79.08	78.01	81.38	79.99	79.00	73.40	71.52	65.50
15	74.07	73.54	76.77	77.06	76.67	81.16	81.15	78.24	72.59	67.92
17	71.41	74.19	78.14	77.17	77.62	81.84	81.82	79.74	76.66	74.01
20	73.08	71.52	76.06	75.40	78.37	83.82	85.81	86.87	78.66	80.33
25	74.87	73.78	77.21	76.29	79.06	83.04	82.16	85.05	89.66	89.03
30	72.48	75.19	72.72	76.05	76.59	81.15	82.40	79.56	87.10	92.42

Table A2. Gust profiles - Terrain Category 2½

Height m	Profile 1	Profile 2	Profile 3	Profile 4	Profile 5	Profile 6	Profile 7	Profile 8	Profile 9	Profile 10
3	63.21	60.38	60.58	58.40	57.07	54.67	53.71	53.21	49.56	48.70
5	64.51	67.55	62.87	59.82	60.86	57.16	57.88	56.42	56.73	50.97
7	64.80	69.87	69.19	67.16	64.40	62.04	62.52	60.82	52.51	53.62
10	65.31	64.99	67.80	70.70	66.74	64.05	67.02	65.15	59.96	60.03
12	72.15	66.11	66.78	72.12	72.22	72.47	71.32	67.13	64.08	59.10
15	65.55	68.37	71.44	70.05	75.44	75.36	77.03	68.64	70.28	67.36
17	67.07	69.62	69.10	74.14	73.02	76.83	75.14	73.29	74.05	69.04
20	68.62	64.87	70.91	73.06	76.68	76.51	78.12	82.15	75.87	70.63
25	65.20	67.78	73.31	71.46	77.50	78.97	75.81	81.43	84.24	83.87
30	71.74	74.05	72.57	72.91	75.77	76.06	80.88	78.85	82.27	88.05

Table A2. Gust profiles - Terrain Category 3

Height m	Profile 1	Profile 2	Profile 3	Profile 4	Profile 5	Profile 6	Profile 7	Profile 8	Profile 9	Profile 10
3	58.98	58.99	51.78	52.66	50.31	49.30	48.54	47.37	47.26	42.85
5	50.96	58.66	55.89	60.24	49.62	45.70	46.36	46.25	47.02	45.86
7	59.28	54.23	55.41	54.49	58.65	58.33	54.50	52.31	48.77	45.93
10	56.63	64.27	60.50	57.66	61.41	58.64	59.33	55.45	53.17	54.24
12	57.82	60.13	62.56	60.99	65.35	58.21	62.16	56.09	58.71	56.21
15	60.51	63.00	64.27	62.52	71.46	69.38	66.75	66.76	63.13	60.30
17	60.89	65.80	65.14	65.47	65.81	72.28	71.10	67.01	65.10	57.31
20	62.97	63.45	66.17	69.30	71.66	71.12	68.24	74.42	73.56	69.75
25	59.36	67.76	65.08	65.38	67.48	75.64	77.83	76.07	78.72	74.52
30	63.15	63.49	66.77	65.72	72.50	70.46	75.62	75.02	80.54	84.39

APPENDIX B

SIMULTANEOUS GUST PROFILES – THUNDERSTORM DOWNDRAFT

Table B1. Gust profiles – downdraft

Height m	Profile 1	Profile 2	Profile 3	Profile 4	Profile 5	Profile 6	Profile 7	Profile 8	Profile 9	Profile 10
3	36.50	37.60	36.58	36.92	35.68	35.32	34.90	34.68	34.21	33.13
5	40.76	41.64	41.07	40.41	40.22	38.60	39.14	37.77	37.87	36.94
7	43.26	42.62	43.76	43.15	42.08	41.90	41.32	40.73	40.33	38.96
10	45.43	45.95	46.64	46.91	46.23	45.42	45.88	44.95	44.40	43.18
12	45.09	45.30	45.92	46.17	47.04	46.61	45.25	45.53	44.24	43.25
15	44.49	44.54	44.80	45.56	45.57	46.84	46.69	45.06	44.09	43.89
17	43.86	44.10	44.78	45.45	45.48	46.44	46.47	46.08	43.90	44.56
20	43.08	43.62	44.24	44.94	44.77	45.50	46.01	46.71	44.66	44.28
25	42.26	42.28	42.99	44.03	43.81	46.07	45.30	45.21	46.87	46.41
30	41.42	41.32	42.12	43.04	43.65	43.29	43.66	44.19	45.66	46.94

APPENDIX C

NORMALIZED GUST ENVELOPE PROFILES – TROPICAL CYCLONE

Table C1. Normalized gust envelope profiles - Terrain Category 2 ($M_{z,Cat\ 2}/M_{10,Cat\ 2}$)

Height m	Profile 1	Profile 2	Profile 3	Profile 4	Profile 5	Profile 6	Profile 7	Profile 8	Profile 9	Profile 10
3	0.908	0.896	0.894	0.933	0.884	0.903	0.886	0.902	0.859	0.927
5	0.995	0.980	0.946	0.986	0.962	1.010	0.978	0.970	0.945	0.990
7	0.994	1.031	1.010	0.986	0.982	0.987	0.959	0.984	0.967	0.998
10	1.000	1.000	1.000	1.000	1.000	1.000	1.000	1.000	1.000	1.000
12	1.056	1.025	1.032	1.033	0.998	1.043	0.997	1.008	1.005	1.027
15	1.058	1.059	1.028	1.069	1.048	1.076	1.016	1.027	1.021	1.039
17	1.092	1.059	1.079	1.060	1.042	1.053	1.046	1.045	1.047	1.102
20	1.110	1.103	1.037	1.068	1.088	1.107	1.068	1.106	1.098	1.103
25	1.145	1.151	1.069	1.091	1.089	1.196	1.126	1.113	1.099	1.142
30	1.245	1.188	1.177	1.178	1.192	1.199	1.179	1.165	1.127	1.203

Table C2. Normalized gust envelope profiles - Terrain Category 2½ ($M_{z,Cat\ 2½}/M_{10,Cat\ 2½}$)

Height m	Profile 1	Profile 2	Profile 3	Profile 4	Profile 5	Profile 6	Profile 7	Profile 8	Profile 9	Profile 10
3	0.911	0.892	0.917	0.896	0.855	0.886	1.002	0.877	0.845	0.869
5	0.915	0.933	0.921	0.968	0.941	1.005	0.959	0.932	0.920	0.971
7	0.970	0.933	1.039	0.955	1.000	0.979	1.013	0.928	0.939	0.968
10	1.000	1.000	1.000	1.000	1.000	1.000	1.000	1.000	1.000	1.000
12	1.043	1.052	1.060	1.012	1.003	1.068	1.064	1.017	0.963	1.048
15	1.057	1.022	1.112	1.057	1.027	1.101	1.098	1.067	1.005	1.040
17	1.086	1.070	1.077	1.111	1.063	1.104	1.095	1.053	1.057	1.121
20	1.141	1.046	1.125	1.109	1.055	1.116	1.174	1.066	1.039	1.164
25	1.241	1.141	1.156	1.199	1.164	1.153	1.273	1.163	1.123	1.204
30	1.292	1.220	1.220	1.186	1.199	1.252	1.255	1.176	1.154	1.250

Table C3. Normalized gust envelope profiles - Terrain Category 3 ($M_{z,Cat\ 3}/M_{10,Cat\ 3}$)

Height m	Profile 1	Profile 2	Profile 3	Profile 4	Profile 5	Profile 6	Profile 7	Profile 8	Profile 9	Profile 10
3	0.960	0.882	0.899	0.919	0.903	0.838	0.903	0.880	0.880	0.851
5	0.936	0.945	0.851	0.954	0.924	0.921	0.903	0.882	0.921	0.904
7	0.989	0.932	1.001	0.949	0.985	0.891	0.931	1.008	0.913	0.884
10	1.000	1.000	1.000	1.000	1.000	1.000	1.000	1.000	1.000	1.000
12	1.018	1.052	1.011	1.064	1.074	0.977	1.031	1.047	1.022	1.036
15	1.109	1.112	1.116	1.118	1.116	1.062	1.132	1.133	1.114	1.020
17	1.181	1.246	1.142	1.193	1.138	1.130	1.142	1.143	1.118	1.137
20	1.218	1.189	1.199	1.178	1.188	1.170	1.161	1.252	1.270	1.150
25	1.208	1.232	1.274	1.306	1.306	1.154	1.209	1.207	1.272	1.278
30	1.320	1.293	1.324	1.348	1.318	1.209	1.216	1.231	1.258	1.262

APPENDIX D

NORMALIZED GUST ENVELOPE PROFILES – THUNDERSTORM DOWNDRAFT

Table D1. Normalized gust envelope profiles – downdraft ($M_{z,Cat}/M_{10,Cat}$)

Height m	Profile 1	Profile 2	Profile 3	Profile 4	Profile 5	Profile 6	Profile 7	Profile 8	Profile 9	Profile 10
3	0.792	0.793	0.799	0.793	0.786	0.800	0.793	0.816	0.801	0.796
5	0.887	0.887	0.892	0.890	0.874	0.896	0.883	0.887	0.861	0.871
7	0.924	0.940	0.927	0.950	0.923	0.931	0.925	0.923	0.927	0.930
10	1.000	1.000	1.000	1.000	1.000	1.000	1.000	1.000	1.000	1.000
12	1.014	0.981	1.002	1.010	0.976	0.986	0.971	1.009	0.980	0.996
15	1.039	0.991	1.008	0.998	1.002	0.991	0.981	1.015	0.991	0.979
17	1.025	0.997	1.016	1.002	0.996	1.005	0.984	1.025	1.005	1.011
20	1.023	1.014	0.988	0.982	0.994	0.983	0.986	0.989	0.989	0.995
25	1.023	0.978	1.009	1.003	1.008	0.985	1.000	1.011	0.992	1.016
30	1.014	0.997	1.015	0.993	0.980	1.003	1.010	0.987	0.963	0.996

APPENDIX E

STATISTICAL PARAMETERS FOR DEBRIS TYPES AND GENERATION

Table E1. Recommended proportions of debris types for Australian suburban conditions

Type	Examples	Proportion (capital cities, ex Darwin)	Proportion (tropical towns)
Compact	Loose nails screws, washers, parts of broken tiles, chimney bricks, air conditioner units	20	15
Sheet/plate	Roof cladding (mainly tiles, steel sheet, flashing, solar panels)	50	45
Rod	Parts of timber battens, purlins, rafters	30	40

Table E2. Recommended mean and coefficients of variation

(a) Capital cities (ex Darwin)

Type	Mass mean (Kg)	Mass c.o.v.	Frontal area mean (m^2)	Frontal area c.o.v.
Compact	0.100	1.0	0.002	0.5
Sheet/plate	3	0.3	0.1	0.3
Rod	4	0.5	0.1	0.3

(b) Provincial towns and cities (incl. Darwin)

Type	Mass mean (Kg)	Mass c.o.v.	Frontal area mean (m^2)	Frontal area c.o.v.
Compact	0.100	1.0	0.002	0.5
Sheet/plate	10	0.5	1	0.3
Rod	4	0.5	0.1	0.3

APPENDIX F

FLOW CHART FOR DEBRIS GENERATION MODEL

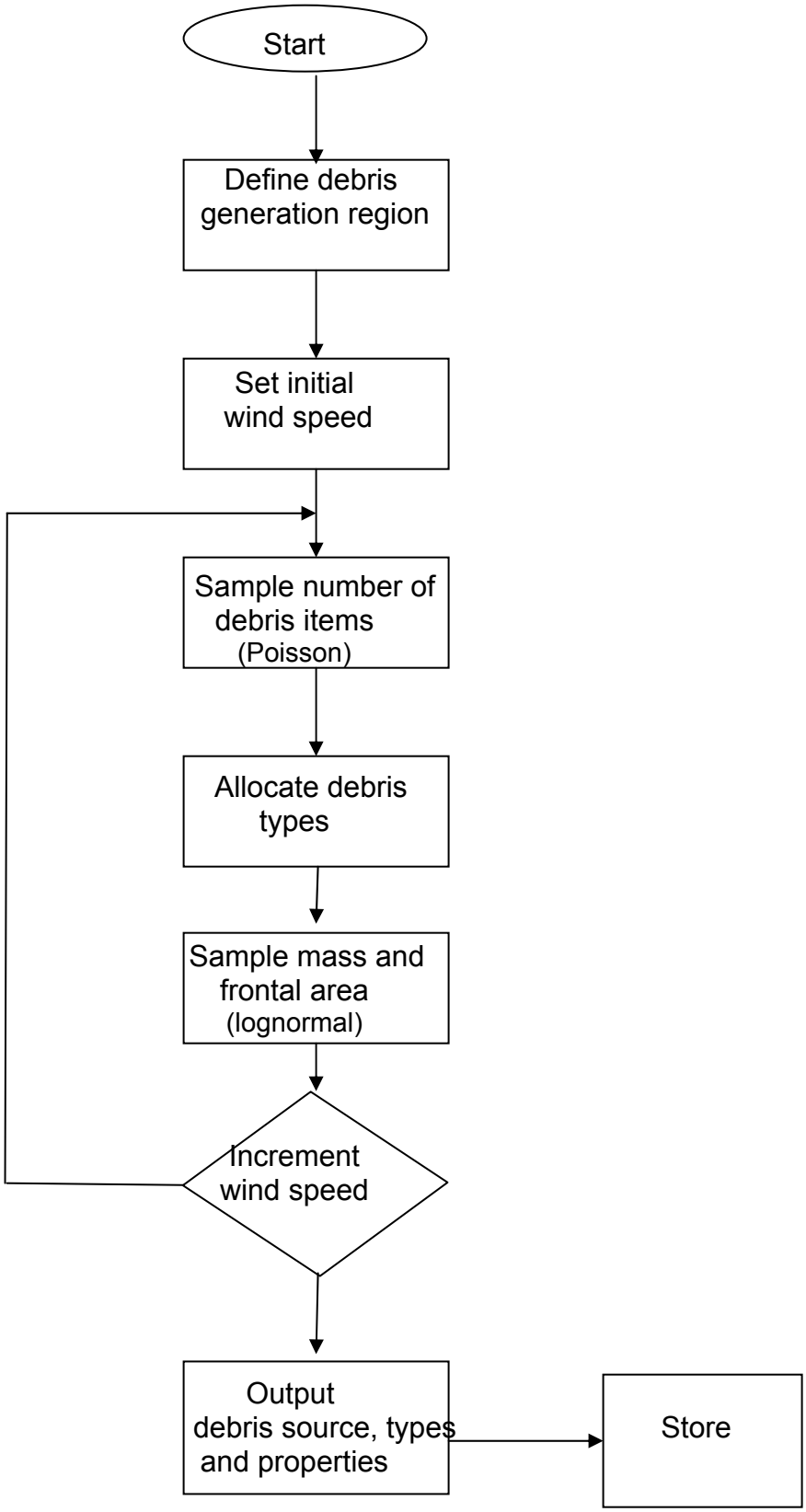
Start
Define debris generation region
Set initial wind speed
Sample number of debris items (Poisson)
Allocate debris types
Sample mass and frontal area (lognormal)
Increment wind speed
Output debris source, types and properties
Store

APPENDIX G

FLOW CHART FOR DEBRIS TRAJECTORIES

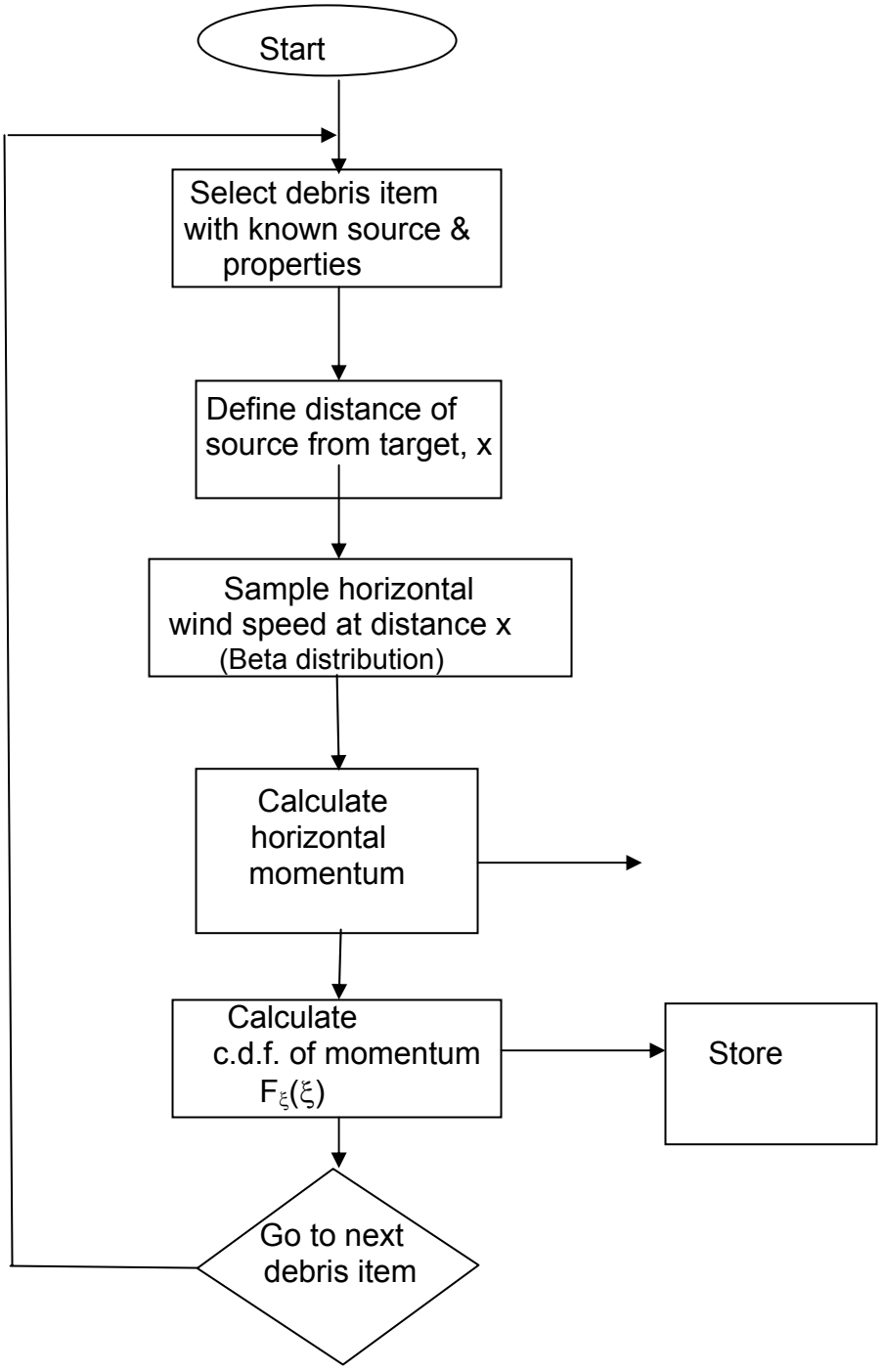
Start
Select debris item with known source & properties
Define distance of source from target, x
Sample horizontal wind speed at distance x (Beta distribution)
Calculate horizontal momentum
Calculate c.d.f. of momentum $F_{\xi}(\xi)$
Store
Go to next debris item

APPENDIX H

FLOW CHART FOR DEBRIS IMPACTS AND DAMAGE CALCULATION

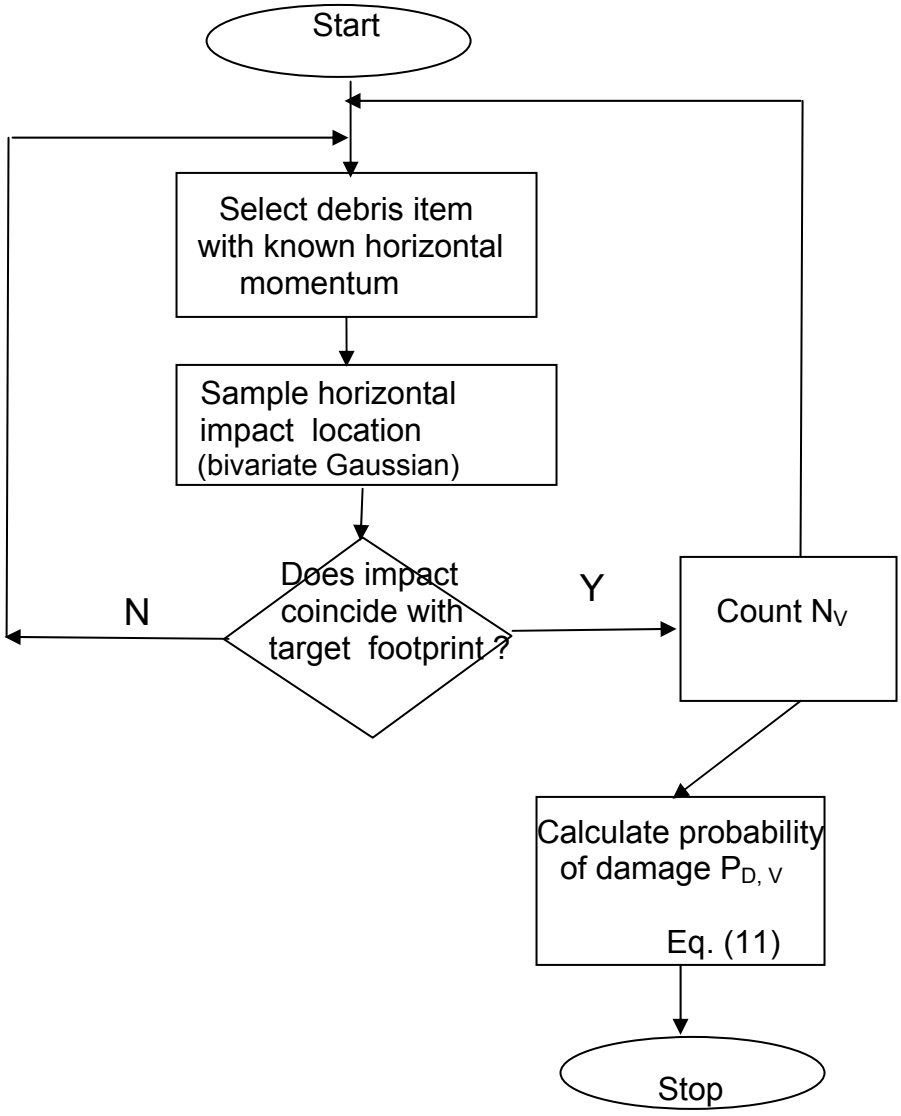
Start
Select debris item with known horizontal momentum
Sample horizontal impact location (bivariate Gaussian)
Does impact coincide with target footprint ?
N
Y
Count N_V
Calculate probability of damage $P_{D, V}$
Eq. (11)
Stop

APPENDIX I

C.V. Dr. J.D. Holmes and JDH Consulting

J.D. HOLMES

Dr. John Holmes is Director, JDH Consulting, Australia. He was previously a Senior Lecturer at James Cook University, Townsville for seven years, at CSIRO, Divisions of Building Research, and Building, Construction and Engineering for fourteen years (reaching the level of Chief Research Scientist), and a Principal Research Fellow at Monash University for five years (all in Australia). In 1989, 2001, 2002 and 2005, respectively, he was a Visiting Professor or Researcher at Texas Tech University, Louisiana State University, University of Western Ontario, Canada, and Texas Tech University (again). In 2003 and 2004 he was John P. Laborde Visiting Professor at Louisiana State University, Baton Rouge, Louisiana, U.S.A., where he studied the mechanics and aerodynamics of windborne debris in hurricanes.

He has been engaged in research, testing and consulting in wind loads and wind effects for more than 30 years. He was actively involved in the writing of Australian Standards AS1170.2-1989, AS/NZS1170.2:2002 (Wind loads) and AS3995-1994 (Design of steel lattice towers and masts), and is currently Chair of Sub-Committee BD006-02 of Standards Australia, responsible for the Australia/New Zealand Wind Actions Standard. He is the author or co-author of some 300 journal papers, conference presentations, and research and consulting reports. He is the author of: "*Wind Loading of Structures*", published by Spon Press of London in 2001, with the second edition published by Taylor and Francis in 2007, and "*A Guide to AS/NZS1170.2:2002 – Wind Actions*" published by Warreen Publishing in 2005. He is an Editor-in-Chief of '*Wind and Structures*', an international journal published by Techno Press, Korea.

He has been a consultant for, or carried out collaborative research with, many companies or organisations. He was awarded a Fulbright Senior Fellowship to the United States in 1989, the Warren Medal by the Institution of Engineers in 1990, and a Senior Fellowship by the Japan Society for Promotion of Science in 1996. He is a Fellow of the Institution of Engineers, Australia and a Life Member of the Australasian Wind Engineering Society, and was formerly an advisor to the Engineering Sciences Data Unit of London, U.K. and to the Technical Committee on Wind Loading of Malaysia. He was Regional Coordinator Asia-Australasia for the International Association for Wind Engineering from 1999 to 2005. He was a consultant for the United Nations Development Program in India in 1994 and 1995, and has represented Australia at ten APEC Structural Loading and Wind Loading Workshops between 1996 and 2009.

He has also been involved in the determination of design wind loads for many major structures including : West Gate Bridge, Melbourne; Citycorp Building, New York; Stadium Australia, Sydney; My Thuan Bridge, Vietnam; Docklands Stadium, Melbourne; Baram Bridge, Malaysia; Macau Tower, China; Wembley Stadium, London; Chevron Redevelopment, Gold Coast, Australia; Woodside offshore platforms, Mauritania, West Africa; Woodside LNG Plant, Western Australia.

JDH CONSULTING

JDH Consulting, founded in 1996, is a specialist engineering consultancy which provides services in the fields of wind engineering, structural dynamics and risk analysis to other consultants, large companies and utilities, universities, and other wind engineering groups. Examples of some of the services provided are as follows:

- Computer analysis of the wind loading on, and dynamic response of, towers, chimneys and masts to wind action
- Assessment reports on environmental wind effects
- Specification of wind pressure coefficients for unusual structural shapes
- Design of structure and foundations for wind loads
- Contract writing of codes, standards and design guides for wind action
- Analysis of historical wind speeds and failure risk of transmission line systems
- Wind-tunnel design
- Supply of advice and equipment for measurement of fluctuating pressures
- Advice, quality assurance and analysis services for wind-tunnel operators, or clients of wind tunnels
- Analysis of wind storm risk
- Expert witness services for failures under wind action
- Delivery of seminars and workshops on wind loading and use of standards

The principal of JDH Consulting is Dr. John D. Holmes

LIST OF CLIENTS OF JDH CONSULTING SINCE 1996

ABB Engineering Construction
ABB-Worley Joint Venture
Ainley-Nixon (structural engineers)
Alan Reay Consultants (NZ)
AMEC Australia Pty. Ltd. (structural engineers)
Arup Pty. Ltd.
Bill Jordan & Associates (structural engineers)
Bluescope Steel
BMT – Fluid Mechanics (U.K.)
Bruce Young Partners (consulting engineers)
Buchanan & Fletcher (structural engineers (N.Z.))
Building Research Association of New Zealand
Bureau of Meteorology – Special Services Unit
Burchill Partners Pty.Ltd.
Burns,Hamilton & Ptnrs. Pty.Ltd.(structural engineers)
Cardno – MBK (NSW) Pty. Ltd.
City University of Hong Kong
Connell Wagner Pty. Ltd. (consulting engineers)
CLP Wind/wave testing facility, Hong Kong University of Science & Technology
CMPS&F (consulting engineers)
Crown Castle International (communication structures)
CSIRO – Division of Building, Construction and Engineering
Cumulus Consulting
Cyclone Testing Station
Dennis Southam & Assoc. (structural engineers)
DLA Phillips Fox (solicitors)
ESDU International (London U.K.)
Electranet (South Australia)
Electricity Supply Association of Australia
Fluor Daniel Ltd.
Gale Pacific Ltd.
Geoscience Australia
G.J.James Australia
Global Environmental Modelling Systems P/L
Glynn Tucker (consulting engineers)
GHD Pty. Ltd. (consulting engineers)
GM Poles Pty. Ltd.
G.P.U. Powernet
Healey and Castle (consulting engineers)
Hong Kong University of Science and Technology
Howard Morley and Assoc.(consulting structural engineers)
I-cubed
James Cook University Cyclone Structural Testing Station
J&H Marsh & McLennan
John H. Van Dyke (developer)Jones and Jones (consulting engineers)
Koukourou Engineers
Larkin-Teys (consulting engineers)
MCS Property Ltd.
Maunsell Australia Pty. Ltd.
Meinhardt (Vic.) Pty. Ltd. (consulting engineers)
Meinhardt (Qld.) Pty. Ltd.(consulting engineers)
MEL Consultants Pty. Ltd.
Middletons, Moore & Bevins (solicitors)
Mott McDonald (consulting engineers, U.K.)
Office of Major Projects (Victoria)
Pacific Solar Pty. Ltd.
Permasteelisa Pty. Ltd.
Peter Blacker & Assoc. (consulting engineer)
Phillips Fox (solicitors)
Powerlink (Queensland)
Qld. Dept. of Public Works and Housing
Radio Frequency Systems Australia (antennas)
Rapcivic Contractors
Raytheon Australia Pty.Ltd.
RED Consultants (Hong Kong)
Research Grants Council, Hong Kong
Roads and Traffic Authority of NSW
Robert Elks & Associates
Rocla Pty.Ltd.
Robert J. Roy (consulting engineer)
Rowell, Forrest & Co.(solicitors)
SAI-Global Ltd.
Saunders Pty.Ltd. (tank manufacturers)
Seminar Services Australia
Standards Australia
Stramit Industries
Structural Engineering Society (New Zealand)
Structures Techne
Suncorp (insurance)
Taperline Australia
TNT Express
Transfield International
University of Western Ontario, Canada
URS Australia
VIPAC Engineers and Scientists
Wallbridge & Gilbert (structural engineers)
Wave Engineering
Weather Solutions Pty Ltd.
Western Power
Weathered Howe - Hyder
Wind Engineering Services – Univ. of Sydney
Windtech Consultants Pty. Ltd.
Woodside Energy Ltd.
Worley-ABB